Automated left atrium boundary detection with intra-cardiac echocardiography during atrial fibrillation ablation

Cristiana Corsi[1], Rachele Angeletti[1], Matteo Zimmitti[2], Corrado Tomasi[3]
[1]DEI, Cesena Campus, University of Bologna, Bologna, Italy; [2]Biosense Webster, Johnson & Johnson Medical s.p.a, Roma, Italy;
[3]Ospedale "S. Maria delle Croci", Ravenna, AUSL della Romagna, Italy

SERVIZIO SANITARIO REGIONALE
EMILIA-ROMAGNA
Azienda Unità Sanitaria Locale della Romagna

Background

Left atrium (LA) posterior wall (LAPW) comprises essential targets for transcatheter radiofrequency ablation (RFA) of atrial fibrillation (AF), but poses problems due to a complex anatomy and to retro-atrial structures potentially damaged by RF, mostly the oesophagus and the related plexi and nerves (1).

Apart from the dreaded atrio-oesophageal fistula, which is fortunately rare (<0.1%) (2), oesophageal lesions have been described in 1.6-28% of cases, and endoscopic mucosal lesions are present in up to 20% of cases (1,3,4).

No preventative method has gained wide acceptance yet. Intracardiac echocardiography (ICE) can be integrated with the 3D electro-anatomical maps constructed by CARTO system (Biosense Webster, Diamond Bar, CA, USA), and can give unique real-time anatomical information about all closely-located peri-cardiac structures [5,6].

In clinical practice, however, the positions of LAPW and oesophagus are monitored by manually tracing ICE images which are transferred onto a 3D electro-anatomical map (Figure 1). This procedure is imprecise, cumbersome and time-consuming, and gives a single static representation of what is a dynamic situation.

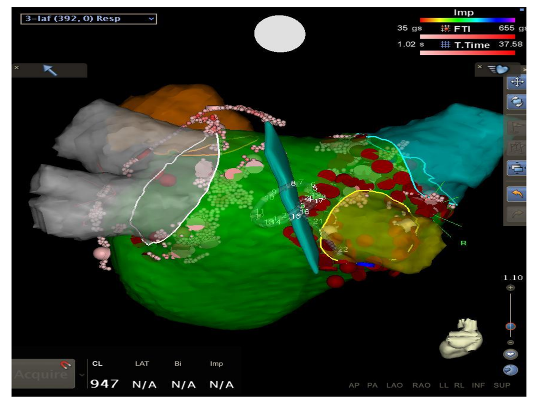

Figure 1. Static 3D reconstruction of LA and oesophagus onto the 3D electro-anatomical map [7].

Aim

The present study aimed to detect LAPW position automatically by ICE during RFA, as a first step to track real-time posterior LA anatomy and retro-atrial spatial 3D relationships.

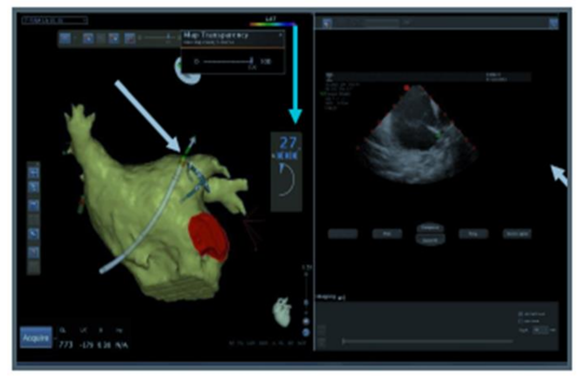

References

[1] Haegeli LM et al., Catheter ablation of atrial fibrillation: an update, Eur Heart J 2014; 35: 454-9.
[2] Nair GM et al., Atrioesophageal fistula in the era of atrial fibrillation ablation: a review, Can. J Cardiol 2014; 30:388–395.
[3] Martinek M et al., Esophageal damage during radiofrequency ablation of atrial fibrillation: impact of energy settings, lesion sets, and esophageal visualization, J Cardiovasc Electrophysiol 2009; 20: 726-33.
[4] Leite LR et al., Luminal esophageal temperature monitoring with a deflectable esophageal temperature probe and intracardiac echocardiography may reduce esophageal injury during atrial fibrillation ablation procedures: results of a pilot study, Circ Arrhythm Electrophysiol 2011; 4: 149-56.
[5] Banchs JE et al., Intracardiac echocardiography in complex cardiac catheter ablation procedures, J Interv Card Electrophysiol, 2010; 28: 167–184.
[6] Filgueiras-Rama D et al., Utility of intracardiac echocardiography for catheter ablation of complex cardiac arrhythmias in a medium-volume training center, Echocardiography, 2015 ;32: 660-70.
[7] Scazzuso FA et al., Three-dimensional esophagus reconstruction and monitoring during ablation of atrial fibrillation: combination of two imaging techniques, Int J Cardiol, 2013 ; 168:2364-8.
[8] Otsu N., A threshold selection method from gray-level histograms, IEEE Trans on Sys Man and Cyber 1979; 9: 62-66.
[9] Chan T et al., Active Contours Without Edges, IEEE Trans Image Process 2001; 10: 266-277.
[10] Hartigan JA et al., A K-Means Clustering Algorithm, Journal of the Royal Statistical Society, Series C, 1979; 28: 100-108.

For additional information: corrado.tomasi@auslromagna.it; cristiana.corsi3@unibo.it

Methods

Image Acquisition

Fourteen ICE sequences were acquired in the Electrophysiology Laboratory of Santa Maria delle Croci Hospital in Ravenna, Italy, during AF ablation procedures. Image sequences were stored on an echographic system (ACUSON Cypress plus, Siemens), then exported in avi format using a magnetic optic device (DynaMO 1300U2, Fujitsu).

Image Analysis

The workflow for LA borders detection is described in figure 2.

Due to the different amount of noise and artifacts in the LA cavity, acquired sequences were divided into two classes: high-noise images, characterized by high presence of noise inside the LA chamber, and low-noise images, characterized by very low noise inside the chamber (Figure 3).

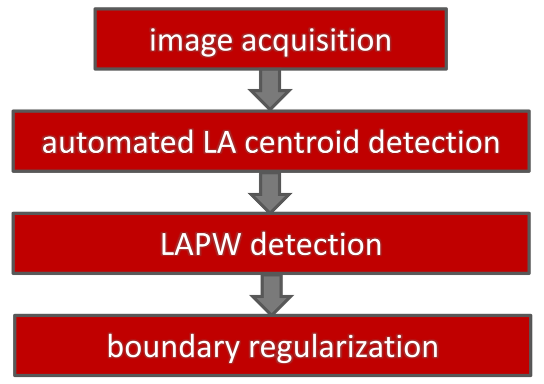

Figure 2. Image analysis workflow

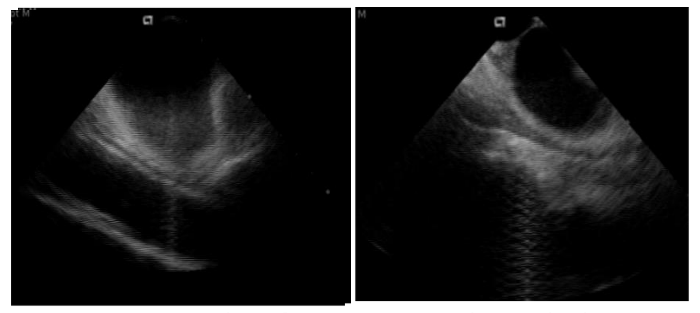

Figure 3. Examples of two images with very high noise (left) and little noise (right).

Two different segmentation methods were developed to detect the LAPW in each class of images.

As a first step for detecting LA boundaries, a mask corresponding to the echo scan was created to limit the working area. Otsu's method [8] was applied to identify the darkest region within the mask. The Otsu method performs an automated thresholding segmentation based on the image histogram. Two-class separation is achieved calculating the optimal threshold by minimizing the intra-class variance (Figure 4B). The region depicting the LA was selected by exploiting LA shape and position knowledge. In this type of acquisition, the LA is typically positioned in the up-right quarter of the echo scan. The centroid of the selected region was then computed (Figure 4C).

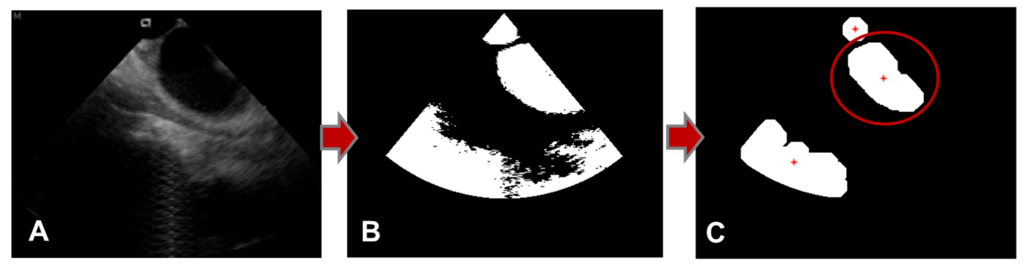

Figure 4. Automated LA centroid detection procedure. A) Original image. B) Mask of the circular sector computed to limit working area. C) Regions detected by applying thresholding segmentation. Red circle indicates the LA region selected by exploiting anatomical information regarding its position.

To detect LA boundaries in images affected by little noise, a procedure based on the region-based level-set Chan-Vese method (CV) [9] was developed. The region-based level-set Chan-Vese method consists in defining a curve in the 2D image space, and letting it evolve by maximizing the differences between the mean gray-level values of the two regions, inside and outside the curve.

The method was applied considering the boundary of the region obtained at the previous step as initial condition (Figure 5A). Result of CV-based segmentation is shown in figure 5B. The LA region was then selected by using the centroid position previously detected and refined by removing "holes", applying erosion and dilatation steps with structural elements of the same size, together with a regularization step (Figure 5C).

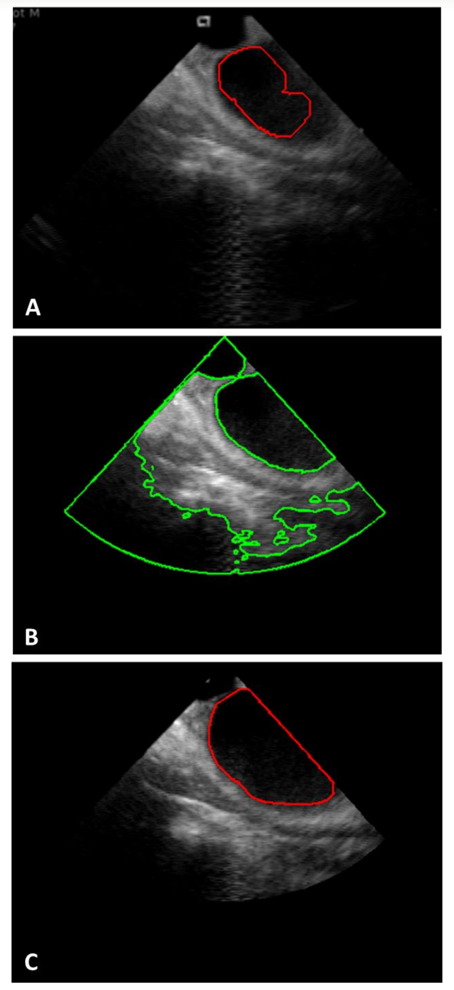

Figure 5. (A) Initial condition and (B) results obtained by applying the CV method; (C) final results after refinement.

To detect LA boundaries in very noisy images a procedure based on clustering K-means algorithm (CL) [10] was developed. The K-means clustering algorithm allows the partition of N observations into k cluster, in which each observation belongs to the "nearest" cluster. The number k of the clusters is *a priori* defined.

Our hypothesis was to differentiate pixels corresponding to blood, cardiac structures and noisy regions by applying a clustering K-means method with k=3. Pixels belonging to the cluster with higher mean gray-level value were considered "cardiac structures"; pixels belonging to the cluster with the lower mean gray-level value were considered "blood" and the remaining pixels belonging to noisy regions (Figure 6).

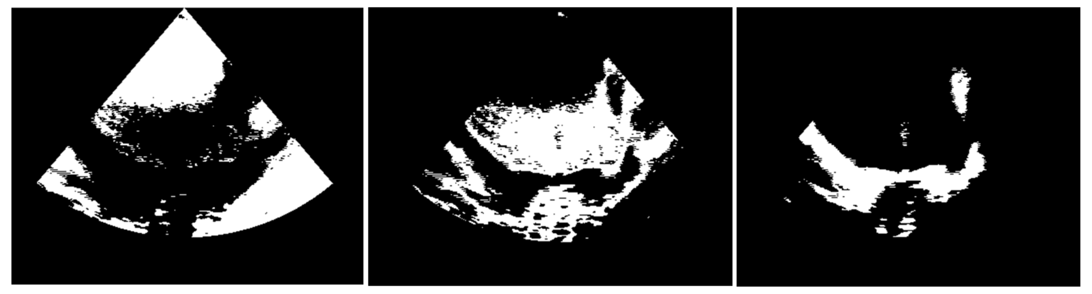

Figure 6. Example of clustering using a K-means algorithm with k=3. On the left panel we show "blood" regions, in the middle panel noisy regions and on the right panel pixels belonging to cardiac structures.

The image was then segmented applying a threshold defined as a weighted average of cluster centers. The resulting detection was refined using morphological operators. The region containing the atrium centroid was selected and dilated with a structural element of the same size as the one used for the erosion. Finally, the detected LA cavity was refined by applying a boundary regularization procedure (Figure 7).

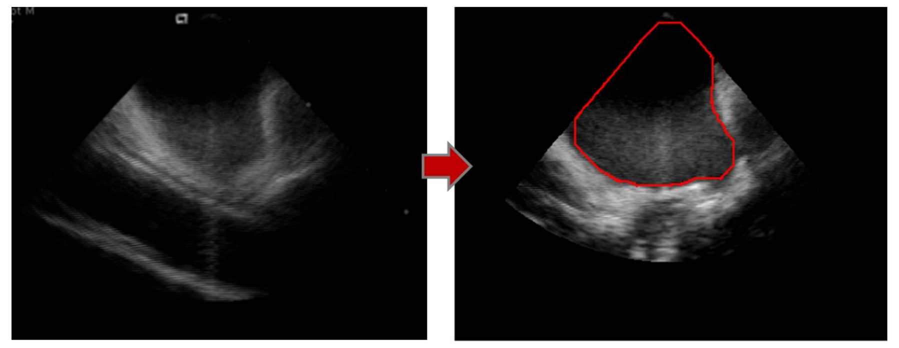

Figure 7. Left panel: original image ; right panel: final result obtained applying the k-means method.

Results

Fourteen ICE sequences were successfully analyzed (9 applying the CV-based method and 5 applying the CL-based technique) for a total of 3058 frames.

Time required for automated analysis on a personal computer was 0.6 and 1.5 sec/frame for CL and CV, respectively.

A success rate was defined with reference to the visual evaluation of the correct LAPW boundary detection. LA boundaries were correctly detected in 83,82% and 83,91% of frames analyzed by CL and CV, respectively.

Two series of detected LA boundaries were compared with manually traced (MT) LA boundaries by an experienced cardiologist by linear regression, Bland-Altman analysis, Dice coefficient (D) and Hausdorff distance (HD).

An example of the comparison between the detected LA contours (in red) and the manually traced LA boundaries by an experienced cardiologist (in green) is shown in figure 8.

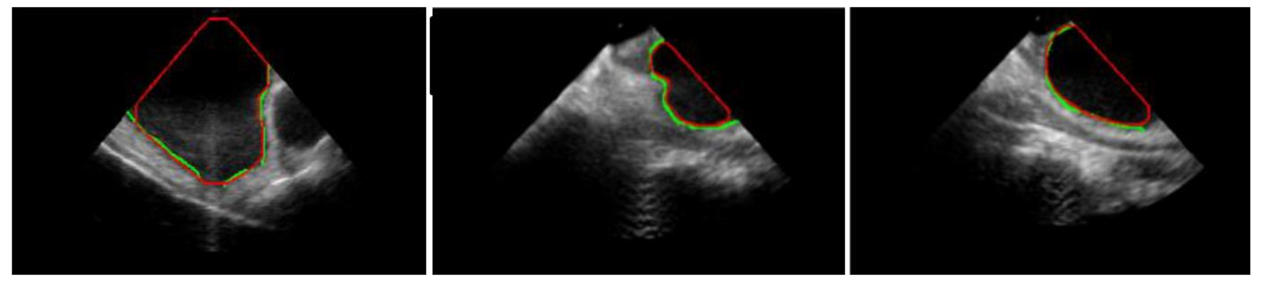

Figure 8. Examples of the comparison between the detected LA contours (in red) and the manually traced LA boundaries by an experienced cardiologist.

Detected contours were in very good agreement with MT (see table):

	Linear regression	Correlation coefficient	Bias (pixels (%))	SD (pixels)	D (mean±SD)	HD (pixels)
CL	y=1.0x-1654	0.92	-1159 (0.73)	1011	0.95±0.029	4.5±0.7
CV	y=0.9x-153	0.99	-827 (0.57)	376	0.94±0.018	4.0±0.6

Additional examples of detected contours in different patients are shown in figure 9.

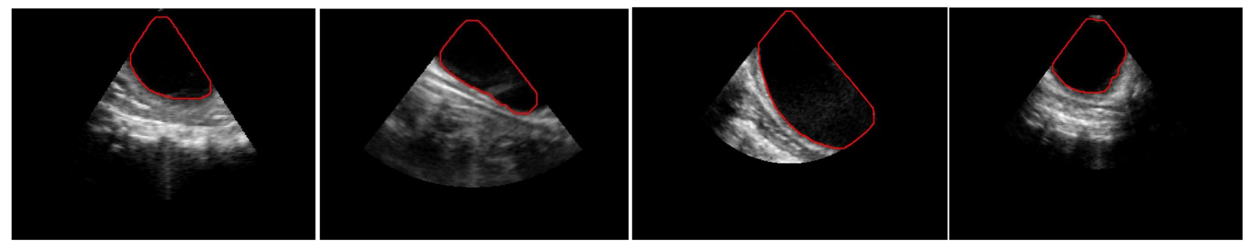

Figure 9. Examples of LA detected contours in different patients.

Conclusion

The proposed algorithm was able to detect LAPW borders accurately and reliably, even with suboptimal quality images. Importantly, the developed procedure for real-time dynamic detection of LA cavity and LAPW is completely automated.

Further validation on a large number of ICE datasets is necessary, hopefully including data in DICOM format.

These preliminary results are promising and may represent the preliminary step for additional LA volumetric reconstruction, including dynamic quantification of esophagus real-time position' changes and its distance from the LAPW during procedure course, to improve AF RFA safety.